Fibrillar Amyloid β-Protein Binds Protease Nexin-2/Amyloid β-Protein Precursor: Stimulation of Its Inhibition of Coagulation Factor XIa†

Matthew R. Wagner, David M. Keane, Jerry P. Melchor, Kenneth R. Auspaker, and William E. Van Nostrand*

Departments of Medicine and Pathology, State University of New York, Stony Brook, New York 11794-8153

Received February 7, 2000; Revised Manuscript Received March 28, 2000

ABSTRACT: Cerebrovascular deposition of fibrillar 39−42 amino acid amyloid β-protein (Aβ), a condition known as cerebral amyloid angiopathy (CAA), is a key pathological feature of Alzheimer's disease and related disorders including hereditary cerebral hemorrhage with amyloidosis-Dutch type (HCHWA-D). Severe cases of CAA, particularly in HCHWA-D, lead to recurrent and often fatal hemorrhagic strokes. Although the reasons for this pathological consequence remain unclear, alterations in proteolytic hemostasis mechanisms have been implicated. For example, the Aβ parent molecule protease nexin-2/amyloid β-protein precursor (PN-2/AβPP), which is elevated in HCHWA-D cerebral vessels with Aβ deposits, is a potent inhibitor of coagulation factor XIa (FXIa). Here we show that fibrillar HCHWA-D Aβ binds PN-2/AβPP, but not its isolated Kunitz-type proteinase inhibitor (KPI) domain, in a saturable, dose-dependent manner with a K_d of ≈28 nM. Neither PN-2/AβPP nor its KPI domain bound to nonfibrillar HCHWA-D Aβ. The fibrillar Aβ binding domain on PN-2/AβPP was localized to residues 18−119. PN-2/AβPP that bound to fibrillar HCHWA-D Aβ immobilized either in plastic wells or on the surface of cultured cerebrovascular smooth muscle cells was active in inhibiting FXIa. Quantitative kinetic measurements revealed that fibrillar HCHWA-D Aβ caused a >5-fold enhancement of FXIa inhibition by PN-2/AβPP. Similar stimulatory effects on FXIa inhibition by PN-2/AβPP were also observed with fibrillar wild-type Aβ. However, fibrillar Aβ had no effect on the inhibition of trypsin by PN-2/AβPP. These findings suggest that fibrillar Aβ deposits in cerebral vessels can effectively localize and enhance the anticoagulant functions of PN-2/AβPP, thereby contributing to a microenvironment conducive to hemorrhaging.

Cerebrovascular deposition of amyloid, also known as cerebral amyloid angiopathy (CAA),[1] is a key pathological feature of Alzheimer's disease and related disorders including hereditary cerebral hemorrhage with amyloidosis-Dutch type (HCHWA-D) (*1*−*5*). The CAA observed in patients with AD and patients with HCHWA-D share a common amyloid subunit known as the amyloid β-protein (Aβ) (*4, 6, 7*). Aβ is a 39−42 amino acid peptide that has the propensity to self-assemble into insoluble, β-sheet-containing fibrils (*7, 8*). Aβ is proteolytically derived from a large transmembrane precursor protein, termed the amyloid β-protein precursor (AβPP), which is encoded by a gene located on chromosome 21 (*9, 10*). Individuals with HCHWA-D have a point mutation in their AβPP gene that results in a glutamine for glutamic acid substitution at position 22 in the Aβ domain (*11*). Full-length AβPP is translated from primarily 3 alternatively spliced mRNAs, resulting in polypeptides of 695, 751, and 770 amino acids: the latter 2 species contain an additional Kunitz-type serine proteinase inhibitor (KPI) domain (*12, 13*).

Secreted 751/770 isoforms of AβPP are analogous to the previously described cell-secreted proteinase inhibitor protease nexin-2 (PN-2) (*14*). In earlier studies, we showed that both purified PN-2/AβPP and its recombinantly expressed KPI domain are tight-binding inhibitors of certain serine proteinases, most notably several enzymes of the blood coagulation cascade including factors XIa, IXa, and Xa (*14*−*18*). Moreover, PN-2/AβPP and its isolated KPI domain can inhibit the clotting of plasma in vitro (*16*). These properties, coupled with the finding that PN-2/AβPP is an abundant, secreted platelet α granule protein, suggest that this protein may have a physiological function in regulating the clotting process at sites of vascular injury (*19*−*22*).

Severe cases of CAA, particularly in HCHWA-D, are characterized by recurrent and often fatal hemorrhagic strokes (*2, 4, 5*). Although the reasons for this pathological consequence remain unresolved, it has been proposed that fibrillar Aβ deposition disrupts the integrity of the vessel wall through the degeneration of cerebrovascular cells leading toward a tendency for vessel rupture (*5, 23, 24*). In addition, there is pathological accumulation of AβPP in the cerebral vessel walls afflicted with Aβ deposition (*25, 26*). The abnormal accumulation of fibrillar Aβ and AβPP in the vessel wall may influence the activity of certain hemostatic proteinases

† This work was supported by National Institutes of Health Grants HL49566 and NS35781 and Research Career Development Award HL03229.

* Address correspondence to this author at the Department of Medicine, HSC T-15/081, State University of New York, Stony Brook, NY 11794-8153. Tel.: 631-444-1661. FAX: 631-444-7518. Email: wevn@mail.som.sunysb.edu.

[1] Abbreviations: CAA, cerebral amyloid angiopathy; Aβ, amyloid β-protein; AD, Alzheimer's disease; HCHWA-D, hereditary cerebral hemorrhage with amyloidosis-Dutch type; PN-2, protease nexin-2; AβPP, amyloid β-protein precursor; FXIa, factor XIa; SDS−PAGE, sodium dodecyl sulfate−polyacrylamide gel electrophoresis; PBS, phosphate-buffered saline; BSA, bovine serum albumin; HCSM cells, human cerebrovascular smooth muscle cells; TBS, Tris-buffered saline.

10.1021/bi0002840 CCC: $19.00
Published on Web 05/27/2000

in a manner that may also contribute to the development of hemorrhages. For example, fibrillar Aβ can potently stimulate the activity of tissue plasminogen activator (*27*, *28*). In addition, the pathological accumulation of PN-2/AβPP, an inhibitor of several key coagulation enzymes, could contribute to an elevated anti-coagulant environment. In this regard, the present study was undertaken to investigate the interactions between fibrillar Aβ and PN-2/AβPP with respect to inhibition of coagulation factor XIa (FXIa). Here we show that fibrillar Aβ mediates the high-affinity binding of PN-2/AβPP and stimulates its ability to inhibit FXIa. These findings suggest that cerebrovascular fibrillar Aβ deposits can localize and enhance the anti-coagulant functions of PN-2/AβPP within the cerebral vessel wall, possibly contributing to the hemorrhagic strokes that are characteristic of CAA.

EXPERIMENTAL PROCEDURES

Materials. HCHWA-D $A\beta_{1-40}$ and wild-type $A\beta_{1-42}$ were synthesized by solid-phase F-moc amino acid chemistry, purified by reverse-phase HPLC, and structurally characterized as previously described (*29*). The lyophilized Aβ peptides were resuspended in sterile distilled water to a concentration of 1 mg/mL immediately prior to use. For preparation of fibrillar Aβ, the peptides were resuspended at a concentration of 10 mg/mL in sterile distilled water and incubated at 37 °C for several days. The β-sheet secondary structure of the fibrillar Aβ peptide preparations was confirmed by circular dichroism spectroscopy and transmission electron microscopy (TEM) as previously described (*30*). The anti-PN-2/AβPP mouse monoclonal antibody (mAb) P2-1, which specifically recognizes an epitope in the amino-terminal region of PN-2/AβPP, was prepared as previously described (*14*). PN-2/AβPP was immunopurified from conditioned cell culture medium as described (*15*). The recombinant KPI domain of PN-2/AβPP was expressed in the *Pichia pastoris* system and purified as described (*31*). Both purified PN-2/AβPP and its KPI domain were biotinylated according to the manufacturer's protocol using the Pierce EZ Sulfo-link Biotin (Rockford, IL). Human factor XIa was obtained from Enzyme Research Laboratories (South Bend, IN). Bovine trypsin was from Sigma (St. Louis, MO). The chromogenic substrates pyro-Glu-Pro-Arg-*p*-nitroanilide (S-2366) and carbobenzoxy-Val-Gly-Arg-*p*-nitroanilide (Chromozym TRY) were purchased from Chromogenix (Westchester, OH) and Roche Biochemicals (Indianapolis, IN), respectively. Secondary peroxidase-coupled sheep anti-mouse IgG was purchased from Amersham (Arlington Heights, IL). Supersignal Dura West chemiluminescence substrate was purchased from Pierce (Rockford, IL).

Cloning, Expression, and Purification of $A\beta PP_{18-119}$ in P. pastoris. Human AβPP exon 2-3 was amplified from AβPP-770 cDNA by PCR using Taq polymerase (Roche Biochemicals) and the primers 5′-CTGGAGGTACCCACTGATAAT-3′ (top strand) and 5′-AACTAAGCAGCGGTAGCGAATCAC-3′ (bottom strand) and inserted into the T-A cloning vector pCR2.1 vector (Invitrogen, San Diego, CA). The integrity of the AβPP exon 2-3 PCR product was confirmed by sequencing. Subsequently, both the amplified product and the *P. pastoris* vector PICZαB (Invitrogen) were cleaved with *Eco*RI, and the fragment was inserted in-frame. The PICZαB vector contains a gene for zeocin antibiotic, and it also carries the AOX1 gene to utilize methanol as its main carbon source. After verification that the insert was in the proper orientation by restriction digest analysis, plasmid DNA was isolated and linearized with *Sac*I. Competent wild-type *P. pastoris* strain X33 was transformed using lithium chloride transformation. To screen clones for high expressors, clones were grown in YPD media with up to 500 μg/mL zeocin and then in BMGY agar plates containing 2 mg/mL zeocin. The high-expressing clones were then inoculated into 25 mL of BMGY media, and the cultures were induced with methanol (to a final concentration of 2%) for 3 days. The yeast cells were pelleted by centrifugation, and the culture supernatant containing secreted $A\beta PP_{18-119}$ was collected. $A\beta PP_{18-119}$ was immunopurified from culture supernatant using a mAbP2-1-Sepharose column (*15*). The recombinant $A\beta PP_{18-119}$ fragment was eluted from the immunoaffinity column with 100 mM ammonium acetate, pH 2.5, frozen, lyophilized, and stored at −70 °C until use.

Solid-Phase Binding Assays. Fifty nanograms of freshly solubilized or fibrillar HCHWA-D $A\beta_{1-40}$ in 100 μL of phosphate-buffered saline (138 mM NaCl, 2.7 mM KCl, 8.1 mM Na_2HPO_4, 1.2 mM KH_2PO_4, pH 7.2) (PBS) was dried down in 96-well microtiter plates (Corning, Cambridge, MA) overnight at 37 °C. Using this coating procedure, equivalent amounts of each form of peptide were retained in the microtiter wells. The wells were rinsed with PBS 3 times and blocked with 100 μL/well of PBS containing 1 mg/mL bovine serum albumin (BSA) for 1 h at room temperature. After rinsing 3 times with PBS, increasing concentrations of biotinylated-PN-2/AβPP, biotinylated-KPI domain, or biotinylated-$A\beta PP_{18-119}$ in PBS containing 0.1 mg/mL BSA were incubated in triplicate (100 μL/well) for 1 h at room temperature. After the wells were rinsed with PBS 3 times, 100 μL of streptavidin-conjugated horseradish peroxidase, at a dilution of 1:800 in PBS containing 0.1 mg/mL BSA, was added for 1 h at room temperature. The binding of the biotinylated ligands was detected using the colorimetric substrate *o*-phenylenediamine dihydrocholride. Briefly, the substrate was diluted in buffer (0.1 M sodium citrate, pH 4.5) to a final concentration of 1 mg/mL. H_2O_2 was added to a final concentration of 0.012% immediately before the addition of 100 μL of the substrate to each microtiter well. The solution was developed for approximately 30 min at room temperature and quenched by the addition of 50 μL of 4 N H_2SO_4 solution to each well. The conversion of the colorimetric substrate was measured at a wavelength of 490 nm using a Molecular Dynamics Vmax kinetic plate reader (Sunnyvale, CA). The theoretical B_{max} and K_d for the binding of PN-2/AβPP or $A\beta PP_{18-119}$ to fibrillar HCHWA-D $A\beta_{1-40}$ were derived using the MacCurve Fit program.

Human Cerebrovascular Smooth Muscle Cell Culture. Primary cultures of human cerebrovascular smooth muscle (HCSM) cells were established and characterized as previously described (*32*). The HCSM cells used in these studies were between passages 4−7 and maintained in 24-well tissue culture dishes with Dulbecco's minimum essential medium containing 10% fetal bovine serum (Gemini Bio-Products, Calabasas, CA), nonessential amino acids, and antibiotics (GibCo, BRL, Grand Island, NY). For experiments, near-confluent cultures of HCSM cells were placed in serum-free medium containing 0.1% BSA overnight prior to treatment. Freshly solubilized HCHWA-D $A\beta_{1-40}$ at a final

concentration of 25 μM was added to the cultures in serum-free medium and incubated at 37 °C for 6 days. Cell viability was monitored using a fluorescent live/dead cell assay (Molecular Probes, Eugene, OR) following the manufacturer's protocol.

TEM Analysis of HCSM Cell-Surface Aβ Fibrils. For analysis of HCHWA-D Aβ_{1-40} cell-surface fibrils, HCSM cells were grown to near-confluence on Transwell membranes (Corning CoStar, Cambridge, MA). The cells were placed in serum-free media containing 0.1% BSA overnight and then incubated in the absence or presence of freshly resuspended HCHWA-D Aβ_{1-40} at a concentration of 25 μM for 6 days. After incubation, the cells were rinsed in PBS 3 times, fixed with 2% paraformaldehyde/2.5% glutaraldehyde for 20 min at room temperature, and then rinsed again with PBS 3 times. The membranes were treated with 2% OsO_4 for 20 min, washed extensively with distilled water, then block-stained with uranyl acetate, extensively rinsed with distilled water, and dehydrated with a graded series of ethanol rinses. The membranes were infiltrated with Spurr's resin, sliced into thin strips, flat-embedded, and cut into 90 μm sections. The sections were viewed with a JEOL 1200 EX transmission electron microscope at 80 kV.

Immunoblotting Analyses of AβPP. Near-confluent cultures of HCSM cells were incubated in the presence or absence of 25 μM HCHWA-D Aβ_{1-40} for 6 days. After incubation, the HCSM cells were rinsed with PBS 3 times, and the cells were solubilized in a lysis buffer containing 50 mM Tris-HCl (pH 7.5), 150 mM NaCl, 1% Triton X-100, 5 mM EDTA, and proteinase inhibitor cocktail (Roche Biochemicals, Indianapolis, IN). The cell lysates were centrifuged at 14000*g* for 10 min to remove insoluble material. Protein concentrations were determined by the method of Bradford (*33*). Cell lysates were stored at −70 °C until analysis. Equivalent aliquots of the cell lysate samples were electrophoresed in nonreducing sodium dodecyl sulfate−10% polyacrylamide gels (SDS−PAGE), and the proteins were electroblotted onto Hybond nitrocellulose membranes (Amersham, Rockford, IL). Unoccupied sites on the membranes were blocked with 5% nonfat milk overnight in PBS with 0.05% Tween-20. The membranes were probed with mAbP2-1 (5 μg/mL) and then incubated with a secondary peroxidase-coupled sheep anti-mouse IgG antibody at a dilution of 1:1000. The peroxidase activity on the membranes was detected using an enhanced chemiluminescence system and analyzed using a Fluor-S Multi-Imager (Bio-Rad Laboratories, Hercules, CA) with the manufacturer's Multi-Analyst software.

FXIa Inhibition Measurements. Microtiter plates containing immobilized Aβ peptides, prepared as described above, were rinsed and then blocked with a solution of 50 mM Tris-HCl, 150 mM NaCl, pH 7.5 (TBS), containing 0.1% BSA for 30 min at room temperature. After rinsing, 100 μL aliquots of TBS/0.01% BSA containing purified PN-2/AβPP or purified KPI domain were added and incubated for 1 h at room temperature. Alternatively, microtiter tissue culture plates containing fixed HCSM cells that were treated with HCHWA-D Aβ_{1-40}, prepared as described above, were blocked with TBS/0.1% BSA. In either case, the wells were then rinsed 3 times and then incubated with TBS/0.01% BSA containing 1 nM FXIa for 1 h at 37 °C. Chromogenic substrate S-2366 was added to a final concentration of 0.5 mM, and the rate of substrate cleavage was measured at an absorbance of 405 nm for 30 min in a kinetic micotiter plate reader.

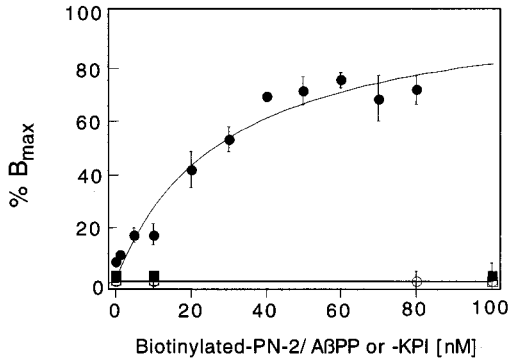

FIGURE 1: Dose-dependent binding of PN-2/AβPP to fibrillar HCHWA-D Aβ_{1-40} in a solid-phase binding assay. Fifty nanograms of soluble or fibrillar HCHWA-D Aβ_{1-40} in 100 μL of PBS was dried down overnight in triplicate wells of a 96-well microtiter plate. After washing, the wells were incubated with increasing concentrations of biotinylated-PN-2/AβPP or biotinylated-KPI domain followed by a streptavidin−horseradish peroxidase conjugate. The binding of biotinylated-ligand was detected using the colorimetric substrate *o*-phenylenediamine dihydrochloride and measured at a wavelength of 490 nm using a Molecular Devices Vmax microplate reader. (●) PN-2/AβPP + fibrillar Aβ; (○) PN-2/AβPP + nonfibrillar Aβ; (■) KPI domain + fibrillar Aβ; (□) KPI domain + nonfibrillar Aβ. Data represent the means ± SD for triplicate samples from two separate experiments. The K_d for the binding of biotinylated-sAβPP to fibrillar HCHWA-D Aβ_{1-40} (28 nM) was calculated using the MacCurve Fit program.

In other experiments, purified PN-2/AβPP (10 nM) was incubated in the absence or presence of increasing concentrations of fibrillar or nonfibrillar Aβ peptides for 30 min at 37 °C. Then FXIa (10 nM) or trypsin (10 nM) was added to the reaction and incubated for an additional 1 h at 37 °C. Chromogenic substrate S-2366 (for FXIa) or Chromozym TRY (for trypsin) was then added to a final concentration of 0.5 mM, and the rate of substrate cleavage was measured at an absorbance of 405 nm for 15 min in a kinetic micotiter plate reader. The inhibition equilibrium constants (K_i) for purified PN-2/AβPP and FXIa in the presence or absence of fibrillar HCHWA-D Aβ_{1-40} were determined by the method of Bieth (*34*) as previously described (*14*, *15*, *31*).

RESULTS

Fibrillar Aβ Binds PN-2/AβPP in a Region Outside of Its KPI Domain. Previous studies have shown that cerebral vessels of HCHWA-D patients containing fibrillar Aβ deposits also exhibit a pathologic accumulation of PN-2/AβPP (*25*). In addition, purified PN-2/AβPP can bind to cerebral vessels that contain fibrillar Aβ (*26*). This suggests that the fibrillar Aβ deposits in these cerebral vessels may mediate the binding of PN-2/AβPP. To directly test this idea, we determined if purified PN-2/AβPP binds to fibrillar and nonfibrillar preparations of HCHWA-D Aβ_{1-40} immobilized in microtiter wells. As shown in Figure 1, biotinylated-PN-2/AβPP exhibited saturable, dose-dependent binding to fibrillar HCHWA-D Aβ_{1-40}. In contrast, no binding was detected with the nonfibrillar form of HCHWA-D Aβ_{1-40}. Additionally, the KPI domain of PN-2/AβPP did not bind to either fibrillar or nonfibrillar HCHWA-D Aβ_{1-40} peptide (Figure 1). This latter finding indicated that the region on

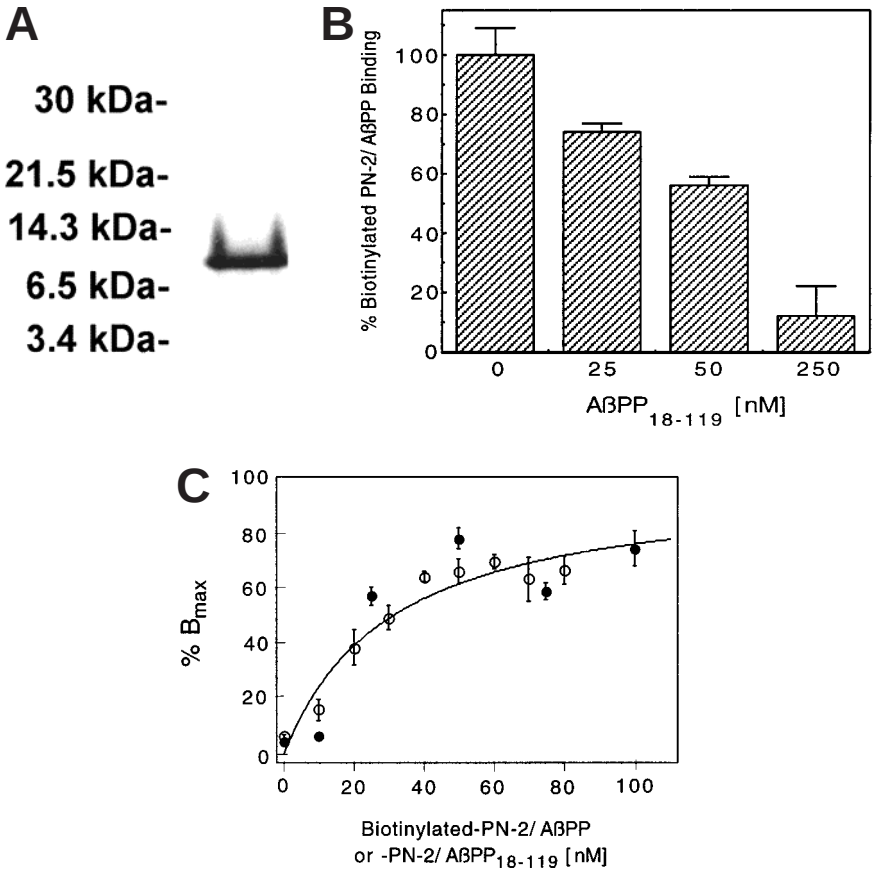

FIGURE 2: Dose-dependent binding of AβPP$_{18-119}$ to fibrillar HCHWA-D Aβ_{1-40} in a solid-phase binding assay. (A) AβPP$_{18-119}$ was recombinantly expressed using the yeast *Pichia pastoris* expression system and was purified by immunoaffinity chromatography as described under Experimental Procedures. Immunopurified AβPP$_{18-119}$ was analyzed by SDS−PAGE and staining with Coomasie Brilliant Blue. (B) Fifty nanograms of fibrillar HCHWA-D Aβ_{1-40} in 100 μL of PBS was dried down overnight in triplicate wells of a 96-well microtiter plate. After washing, the wells were incubated with 50 nM biotinylated-PN-2/AβPP in the absence or presence of increasing concentrations of AβPP$_{18-119}$ followed by a streptavidin−horseradish peroxidase conjugate. The binding of biotinylated-PN-2/AβPP was detected using the colorimetric substrate *o*-phenylenediamine dihydrochloride and measured at a wavelength of 490 nm using a Molecular Devices Vmax microplate reader. Data represent the mean ± SD from quadruplicate samples from two independent experiments. The concentrations of AβPP$_{18-119}$ are: lane 1, 0; lane 2, 25 nM; lane 3, 50 nM; lane 4, 250 nM. (C) Fifty nanograms of fibrillar HCHWA-D Aβ_{1-40} in 100 μL of PBS was dried down overnight in triplicate wells of a 96-well microtiter plate. After washing, the wells were incubated with increasing concentrations of biotinylated-PN-2/AβPP (○) or biotinylated-AβPP$_{18-119}$ (●) followed by a streptavidin−horseradish peroxidase conjugate. The binding of biotinylated-PN-2/AβPP was detected using the colorimetric substrate *o*-phenylenediamine dihydrochloride and measured at a wavelength of 490 nm using a Molecular Devices Vmax microplate reader. Data represent the means ± SD for triplicate samples from two separate experiments. The K_d for the binding of AβPP$_{18-119}$ to fibrillar HCHWA-D Aβ_{1-40} (28 nM) was calculated using the MacCurve Fit program.

PN-2/AβPP responsible for its binding to fibrillar HCHWA-D Aβ_{1-40} resides outside the KPI domain.

A number of ligand binding domains on PN-2/AβPP have been localized within the amino-terminal region of the protein upstream from the KPI domain (*35*−*37*). To further define the region on PN-2/AβPP responsible for its binding to fibrillar HCHWA-D Aβ_{1-40}, we expressed AβPP amino-terminal fragments as free secreted proteins using the yeast *P. pastoris* expression system (*38*). The AβPP amino-terminal fragments were screened for their ability to block biotinylated-PN-2/AβPP binding to fibrillar HCHWA-D Aβ_{1-40} using the solid-phase binding assay described above. The *P. pastoris* expressed fragment AβPP$_{18-119}$, encoded by AβPP exons 2−3, was purified by immunoaffinity chromatography using mAbP2-1 (*15*). The purified AβPP$_{18-119}$ migrated at ≈10 kDa on SDS−PAGE (Figure 2A). Purified AβPP$_{18-119}$ retained the ability to block biotinylated-PN-2/AβPP binding to fibrillar Aβ (Figure 2B). However, neither exon 2 nor exon 3 expressed alone exhibited any competing activity, suggesting that both exons are required for formation of an active fibrillar Aβ binding domain (data not shown). This observation is consistent with a recent report showing that this particular region of sAβPP possesses three disulfide bonds and is highly structured (*39*). Since we identified that AβPP$_{18-119}$ can compete for intact PN-2/AβPP binding to fibrillar HCHWA-D Aβ_{1-40}, we next measured its binding to the same type of fibrillar Aβ using the same solid-phase binding assay. Biotinylated-AβPP$_{18-119}$ also exhibited dose-dependent and saturable binding toward fibrillar HCHWA-D Aβ_{1-40} with a $K_d \approx 28$ nM (Figure 2C), virtually the identical result obtained for biotinylated-PN-2/AβPP binding to fibrillar HCHWA-D Aβ_{1-40}.

PN-2/AβPP Bound to Fibrillar HCHWA-D Aβ$_{1-40}$ Is Functionally Active toward Inhibiting Coagulation FXIa. The above findings indicated that fibrillar Aβ strongly binds PN-2/AβPP. We next wanted to determine if PN-2/AβPP retained its ability to inhibit proteinases while bound to fibrillar Aβ. Coagulation FXIa was chosen since this proteinase is potently inhibited by PN-2/AβPP (*15*, *40*), and elevated levels of PN-2/AβPP−FXIa complexes have been detected in HCHWA-D

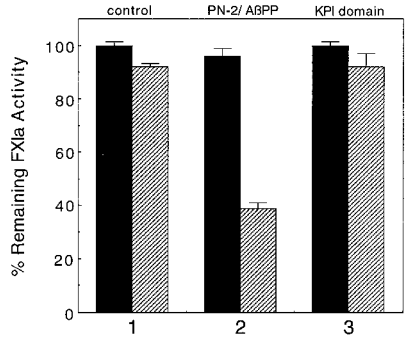

FIGURE 3: PN-2/AβPP bound to immobilized fibrillar HCHWA-D Aβ_{1-40} is functionally active in inhibiting coagulation FXIa. One microgram of fibrillar HCHWA-D Aβ_{1-40} in 100 μL of TBS (hatched bars) or 100 μL of TBS alone (black bars) was dried down overnight in triplicate wells of a 96-well microtiter. After washing, the triplicate wells were incubated with a 100 μL of TBS containing 100 nM PN-2/AβPP or KPI domain for 1 h at 37 °C. After washing, the wells were incubated with 100 μL of TBS containing 1 nM FXIa for 1 h at 37 °C. Then 50 μL of TBS containing 1.5 mM of the FXIa chromogenic substrate S-2366 was added, and the rate of substrate hydrolysis was measured at a wavelength of 405 nm using a Molecular Devices Vmax microtiter plate reader. Data represent the means ± SD for triplicate samples from two independent experiments. Lanes 1, no inhibitor control; lanes 2, PN-2/AβPP; lanes 3, KPI domain.

patients (*41*). Figure 3 shows that in the presence of fibrillar HCHWA-D Aβ_{1-40}, PN-2/AβPP was retained and appreciable FXIa activity was observed (lane 2). Although the KPI domain is a potent inhibitor of FXIa (*31*), no inhibition was observed because of its lack of binding to fibrillar Aβ (lane 3). This demonstrated that fibrillar Aβ can bind and localize PN-2/AβPP with its proteinase inhibitory properties intact.

We next examined the FXIa inhibitory function of PN-2/AβPP in the presence of fibrillar Aβ in a relevant cell culture paradigm. Smooth muscle cells within the cerebral vessel wall are the site of fibrillar Aβ deposition in CAA (*24*−*26*). We recently showed that HCHWA-D Aβ_{1-40} forms fibrils on the surface of cultured HCSM cells and mediates the pathological accumulation of PN-2/AβPP (*30*). The assembly of HCHWA-D Aβ_{1-40} fibrils on the surface of HCSM cells is visualized by TEM analysis (Figure 4B). A subsequent pathological response is the robust binding of endogenous PN-2/AβPP to the Aβ fibrils and its subsequent accumulation on the surface of the HCSM cells (Figure 4C,D). As shown in Figure 4E, the accumulation of endogenous HCSM cell PN-2/AβPP on its cell surface via the assembled HCHWA-D Aβ_{1-40} fibrils resulted in increased inhibition of FXIa. Together, these data indicate that PN-2/AβPP bound to HCHWA-D Aβ_{1-40} fibrils can functionally inhibit FXIa. Furthermore, the latter findings show an elevated FXIa-inhibiting environment present at the surface of HCSM cells treated with HCHWA-D Aβ_{1-40}.

Fibrillar Aβ Enhances the Inhibition of FXIa by PN-2/AβPP. Since fibrillar Aβ can bind and localize PN-2/AβPP, we sought to determine if this interaction alters the efficiency of PN-2/AβPP proteinase inhibitory function. Purified PN-2/AβPP was incubated in the absence or presence of increasing concentrations of freshly resuspended nonfibrillar or fibrillar HCHWA-D Aβ_{1-40}. As shown in Figure 5A, increasing concentrations of fibrillar HCHWA-D Aβ_{1-40} stimulated the ability of PN-2/AβPP to inhibit FXIa. Maximum stimulation was achieved at ≈25 μg/mL fibrillar HCHWA-D Aβ_{1-40}, resulting in a lowering of the K_i from 150 to 28 pM. In contrast, increasing concentrations of nonfibrillar HCHWA-D Aβ_{1-40} had no effect on the ability of PN-2/AβPP to inhibit FXIa. Importantly, under the concentrations used in these experiments, neither nonfibrillar nor fibrillar HCHWA-D Aβ_{1-40} affected the enzymatic activity of FXIa in the absence of PN-2/AβPP (data not shown).

We next investigated the specificity of this stimulatory effect on the proteinase inhibitory properties of PN-2/AβPP. As shown in Figure 5B, increasing concentrations of fibrillar HCHWA-D Aβ_{1-40} did not enhance the ability of PN-2/AβPP to inhibit trypsin. This indicates that stimulation of PN-2/AβPP inhibitory activity is not a general effect but appears restricted to certain target proteinases. In the above studies, we used fibrillar HCHWA-D Aβ_{1-40} which contains the E22Q substitution. To exclude the possibility that these findings are due to the HCHWA-D mutant form of Aβ, we performed studies using fibrillar wild-type Aβ. Figure 5B shows that fibrillar wild-type Aβ_{1-42} exhibits a nearly identical stimulatory effect on PN-2/AβPP inhibition of FXIa. Similarly, increasing concentrations of fibrillar wild-type Aβ_{1-42} did not enhance the ability of PN-2/AβPP to inhibit trypsin (data not shown). This indicates that the structure of the Aβ fibril is responsible for its binding to PN-2/AβPP and stimulation of its inhibition of FXIa.

DISCUSSION

Severe cases of CAA, such as those found in HCHWA-D, are characterized by cerebrovascular deposition of fibrillar Aβ and accompanied by abnormal accumulations of PN-2/AβPP (*1*, *2*, *24*−*26*). The reason as to why PN-2/AβPP collects under these conditions and what the consequences are of this pathological accumulation remain unclear. In the present study, we show that fibrillar Aβ mediates the high-affinity binding of PN-2/AβPP but not its KPI domain. It is of interest that this interaction requires fibrillar Aβ, the predominant form found in CAA, since the nonfibrillar form of Aβ was incapable of binding PN-2/AβPP or its isolated KPI domain (Figure 1). This newly identified fibrillar Aβ binding domain appears to reside in the amino-terminal region of PN-2/AβPP. This was supported by the finding that the recombinantly expressed amino-terminal fragment AβPP$_{18-119}$ retained the ability to compete for PN-2/AβPP binding to fibrillar Aβ (Figure 2B). Moreover, the AβPP$_{18-119}$ fragment exhibited essentially the same binding properties to fibrillar Aβ as did intact PN-2/AβPP (Figure 2C). However, expressing smaller recombinant amino-terminal fragments of AβPP failed to yield an active fibrillar Aβ binding fragment. Recently, the crystal structure has been reported for a similar region of the AβPP molecule, AβPP$_{28-123}$ (*39*). This analysis has revealed the amino-terminal region of AβPP is highly structured, containing three disulfide bonds, high β-strand content, and one α-helix. Therefore, the smaller amino-terminal fragments of AβPP were likely deficient in possessing the correct conformation of an active fibrillar Aβ binding domain. Future site-directed mutagenesis studies are planned to further define the precise site within AβPP$_{18-119}$ that is responsible for binding fibrillar Aβ. Together, these findings suggest that fibrillar Aβ deposits

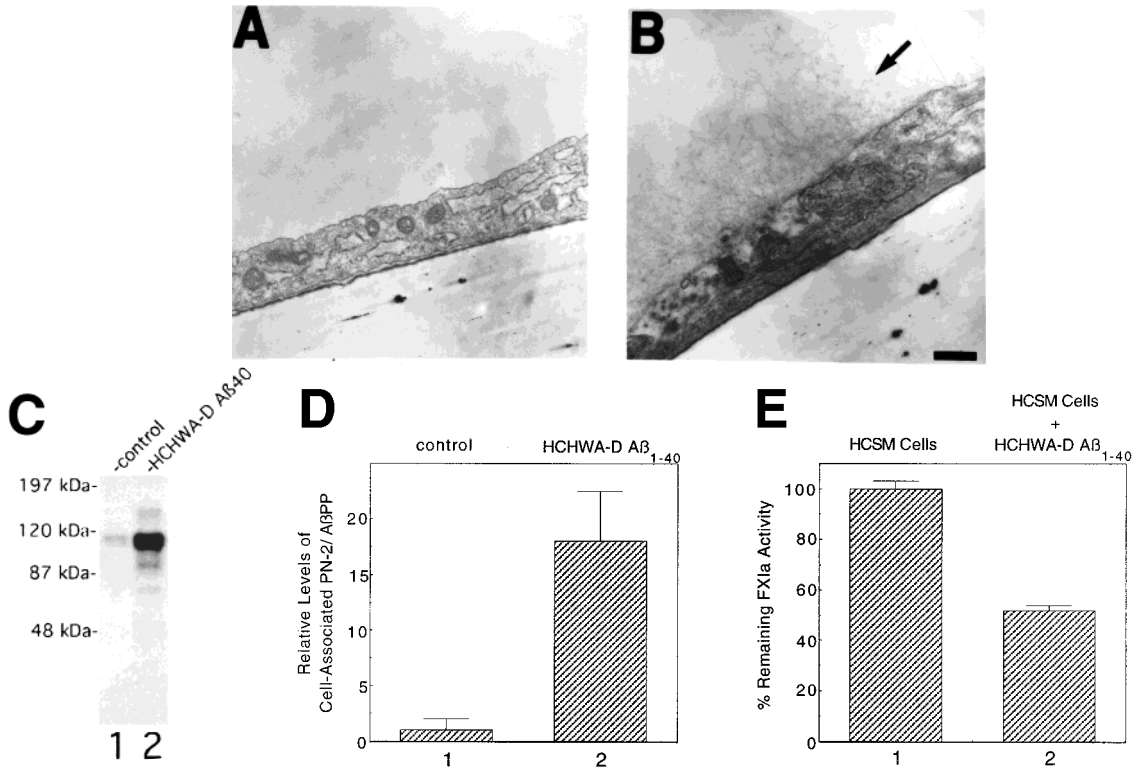

FIGURE 4: PN-2/AβPP bound to HCSM cell-surface fibrillar HCHWA-D $A\beta_{1-40}$ is functionally active in inhibiting coagulation of FXIa. (A and B) Near-confluent cultures of HCSM cells grown on Transwell membranes were incubated in the absence (A) or presence (B) of 25 μM HCHWA-D $A\beta_{1-40}$ for 6 days. The cells were rinsed, fixed, and prepared for TEM analysis as described under Experimental Procedures. The samples were viewed with a JEOL 1200 EX transmission electron microscope at 80 kV under identical conditions. Scale bar = 0.25 μm. The arrow points to the extensive Aβ fibrils on the cell surface. (C and D) Near-confluent cultures of HCSM cells were incubated in the absence (lanes 1) or presence (lanes 2) of 25 μM HCHWA-D $A\beta_{1-40}$ for 6 days. (C) After 6 days, the culture medium was removed, and the HCSM cells were rinsed, solubilized, subjected to SDS−PAGE, and subsequently analyzed for PN-2/AβPP by immunoblotting using mAbP2-1 as described under Experimental Procedures. (D) The relative levels of HCSM cell-surface-associated PN-2/AβPP were determined by quantitative immunoblotting as described under Experimental Procedures. The data presented are the mean ± SD of six separate determinations and expressed as fold increase over control levels. (E) Near-confluent cultures of HCSM cells were grown in 96-well plates and incubated in the absence (lane 1) or presence (lane 2) of 25 μM HCHWA-D $A\beta_{1-40}$ for 6 days. The cells were rinsed, fixed, and incubated with 100 μL of TBS containing 1 nM FXIa for 1 h at 37 °C. Then 50 μL of TBS containing 1.5 mM of the FXIa chromogenic substrate S-2366 was added, and the rate of substrate hydrolysis was measured at a wavelength of 405 nm using a Molecular Devices Vmax microtiter plate reader. Data represent the means ± SD for triplicate individual samples from two independent experiments.

in CAA may mediate the high-affinity binding of PN-2/AβPP in the cerebral vessel wall.

PN-2/AβPP bound to immobilized fibrillar Aβ retained its ability to inhibit coagulation FXIa (Figure 3). This observation indicates that when PN-2/AβPP is bound to fibrillar Aβ through its amino-terminal 18−119 region, its KPI domain is accessible to target proteinases. To investigate this property in a setting more biologically relevant to CAA, we examined the inhibition of FXIa by PN-2/AβPP bound to fibrillar Aβ in our HCSM cell culture paradigm. When pathogenic forms of Aβ are added to HCSM cells in culture, they assemble into an elaborate network of fibrils on the surfaces of these cells (Figure 4B). We have previously shown that these cell-surface fibrils mediate the binding and marked accumulation of endogenous PN-2/AβPP on the HCSM cells, eventually leading to cell death (*30*, *42*−*44*). Here we show that the accumulation of HCSM cell PN-2/AβPP mediated by fibrillar Aβ (Figure 4C,D) results in increased inhibition of FXIa at the cell surface (Figure 4E). This suggests that PN-2/AβPP bound to fibrils on the surfaces of cerebrovascular cells, as observed in HCHWA-D and severe cases of CAA, can functionally inhibit coagulation FXIa.

Although PN-2/AβPP bound to fibrillar Aβ was functionally active in inhibiting FXIa, it was unclear if fibrillar Aβ binding modulated the efficiency of this inhibition. Indeed, fibrillar Aβ was found to exert a dose-dependent enhancement of FXIa inhibition by PN-2/AβPP (Figure 5A). This was due to the binding of fibrillar Aβ to PN-2/AβPP since freshly resuspended nonfibrillar Aβ, which exhibits no binding to PN-2/AβPP (Figure 1), had no effect on the inhibition of FXIa. Additionally, in these experiments neither freshly resuspended nonfibrillar Aβ nor fibrillar Aβ had any effect on the enzymatic activity of FXIa (data not shown). The maximum stimulatory effect was achieved at ≈25 μg/mL fibrillar Aβ. An identical stimulatory effect was observed with both fibrillar HCHWA-D mutant $A\beta_{1-40}$ and fibrillar wild-type $A\beta_{1-42}$, indicating that it is the β-sheet fibrillar structure of Aβ, not the presence of HCHWA-D E22Q substitution, that is responsible for the binding and stimulation of PN-2/AβPP. Either form of fibrillar Aβ increased the potency of FXIa inhibition by PN-2/AβPP greater than 5-fold (Figure 5). This is very similar to the level of stimulation that heparin exerts on the inhibition of FXIa by PN-2/AβPP (*15*). It is noteworthy that the binding domains for heparin and Zn^{2+} also reside in the amino-terminal region

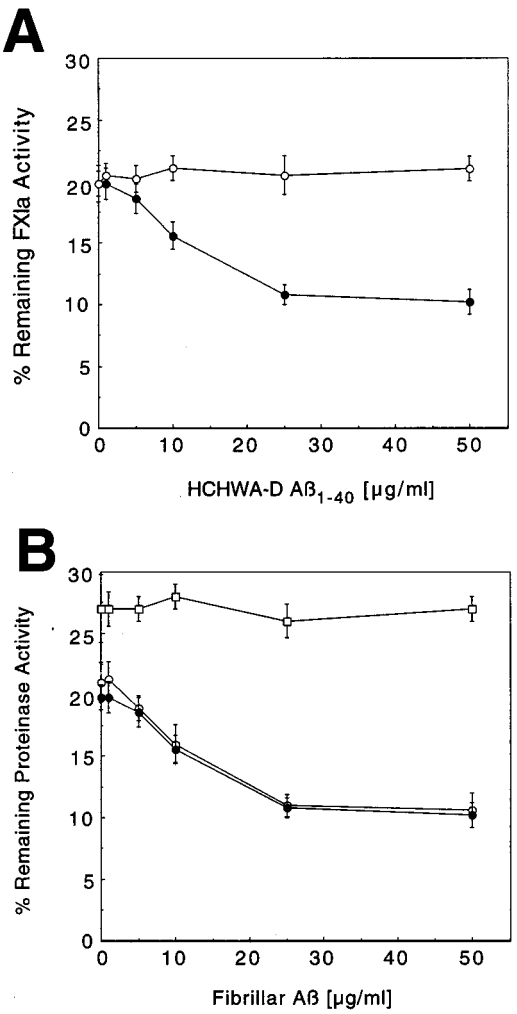

FIGURE 5: Fibrillar Aβ stimulates PN-2/AβPP to inhibit coagulation of FXIa. (A) Increasing concentrations of fibrillar (●) or freshly resuspended (○) nonfibrillar HCHWA-D Aβ_{1-40} were incubated in the presence of 20 nM PN-2/AβPP in 50 μL of TBS for 30 min at 37 °C. Then 50 μL of a 20 nM solution of FXIa in TBS was added to each well and incubated for an additional 1 h at 37 °C. Then 50 μL of TBS containing 1.5 mM of the FXIa chromogenic substrate S-2366 was added, and the rate of substrate hydrolysis was measured at a wavelength of 405 nm using a Molecular Devices Vmax microtiter plate reader. The data are presented as percent remaining FXIa enzymatic activity where 100% is the activity of FXIa in the absence of PN-2/AβPP. Data for each point represent the means ± SD for individual triplicate samples from three independent experiments. (B) Increasing concentrations of fibrillar HCHWA-D Aβ_{1-40} or fibrillar wild-type Aβ_{1-42} were incubated in the presence of 20 nM PN-2/AβPP in 50 μL of TBS for 1 h at 37 °C. Then 50 μL of a 20 nM solution of FXIa or trypsin in TBS was added and incubated for an additional 1 h at 37 °C. Finally, 50 μL of TBS containing 1.5 mM of the FXIa chromogenic substrate S-2366 or the trypsin chromogenic substrate Chromozym TRY was added, and the rate of substrate hydrolysis was measured at a wavelength of 405 nm using a Molecular Devices Vmax microtiter plate reader. (●) FXIa + fibrillar HCHWA-D Aβ_{1-40}; (○) FXIa + wild-type Aβ_{1-42}; (□) trypsin + fibrillar HCHWA-D Aβ_{1-40}. Data represent the means ± SD for individual triplicate samples from three independent experiments.

of PN-2/AβPP (*35*, *36*) and these two factors also enhance the inhibition of FXIa by PN-2/AβPP (*15*, *40*). This suggests that ligands which bind to this general amino-terminal region of PN-2/AβPP can influence its FXIa inhibitory properties. Although the inhibition of FXIa by PN-2/AβPP was enhanced by fibrillar Aβ, the inhibition of trypsin activity was not (Figure 5B). This indicates that the stimulatory effect of PN-2/AβPP FXIa inhibitory properties is not a general effect and is likely restricted to specific target proteinases. Similar findings were previously observed with the stimulatory effects of heparin or Zn^{2+} on PN-2/AβPP proteinase inhibitory properties (*15*, *40*). Together, these studies demonstrate that fibrillar Aβ binding can augment the inhibition of coagulation FXIa by PN-2/AβPP.

The reasons why severe CAA often results in cerebral hemorrhage are still unresolved. However, degeneration and loss of smooth muscle cells and their replacement with Aβ fibrils have been proposed to contribute to the loss of vessel wall integrity (*23*−*26*). In this regard, previous studies have suggested that cerebrovascular Aβ deposits cause smooth muscle cell degeneration in vivo (*1*, *23*−*26*). Further supporting this notion, our recent cell culture studies indicate that pathogenic forms of Aβ can induce apoptotic cell death and other pathologic responses, including marked increases in PN-2/AβPP, in HCSM cells (*42*−*45*). These in vitro cellular pathologic responses clearly involve the assembly of Aβ into cell-surface fibrils (*30*). This is consistent with the correlation between the fibrillar Aβ deposition, cerebrovascular cytotoxicity, and the pathological accumulation of PN-2/AβPP that is observed in HCHWA-D and severe CAA.

In addition to smooth muscle cell degeneration, alterations in proteolytic hemostatic mechanisms may also contribute to the development of cerebral hemorrhage in CAA. For example, previous studies have shown that fibrillar forms of Aβ can potently stimulate the activity of tissue type plasminogen activator (*27*, *28*). This could result in activation of plasminogen at sites of cerebrovascular fibrillar Aβ deposition. Plasmin that is generated can either directly (*46*) or indirectly, through activation of matrix metalloproteinases (*47*, *48*), proteolytically degrade extracellular matrix components. This could significantly undermine the integrity of the vessel wall. The present findings suggest that in CAA cerebrovascular fibrillar Aβ deposits may mediate the binding and accumulation of PN-2/AβPP. Moreover, when bound to fibrillar Aβ, PN-2/AβPP may exhibit elevated inhibition of coagulation FXIa. The pathological accumulation of PN-2/AβPP may exacerbate any loss of vessel wall integrity by providing an elevated anti-coagulant environment, thereby contributing to the hemorrhaging process.

REFERENCES

1. Vinters, H. V. (1987) *Stroke 18*, 311−324.
2. Feldmann, E. (1991) *Stroke 22*, 684−691.
3. Glenner, G. G., Henry, J. H., and Fujihara, S. (1981) *Ann. Pathol. 1*, 120−129.
4. van Duinen, S. G., Castano, E. M., Prelli, F., Bots, G. T. A. M., Luyendijk, W., and Frangione, B. (1987) *Proc. Natl. Acad. Sci. U.S.A. 84*, 5991−5994.
5. Wattendorff, A. R., Frangione, B., Luyendijk, W., and Bots, G. T. A. M. (1995) *J. Neurol., Neurosurg. Psychiatry 59*, 699−705.
6. Glenner, G. G., and Wong, C. W. (1984) *Biochem. Biophys. Res. Commun. 122*, 885−890.
7. Prelli, F., Castano, E., Glenner, G. G., and Frangione, B. (1988) *J. Neurochem. 51*, 648−651.
8. Masters, C. L., Simms, G., Weinman, N. A., Multhaup, G., McDonald, B. L., and Beyreuther, K. (1985) *Proc. Natl. Acad. Sci. U.S.A. 82*, 4245−4269.
9. Selkoe, D. J. (1996) *J. Biol. Chem. 271*, 18295−18298.

10. Yankner, B. A. (1996) *Neuron 16*, 921−932.
11. Levy, E., Carman, M. D., Fernandez-Madrid, I. J., Power, M. D., Lieberburg, I., van Duinen, S. G., Bots, G. T. A. M., Luyendijk, W., and Frangione, B. (1990) *Science 248*, 1124−1126.
12. Ponte, P., Gonzalez-DeWhitt, P., Schilling, J., Miller, J., Hsu, D., Greenberg, B., Davis, K., Wallace, W., Lieberburg, I., Fuller, F., and Cordell, B. (1988) *Nature 331*, 525−527.
13. Tanzi, R. E., McClatchey, A. I., Lamperti, E. D., Villa-Komaroff, L., Gusella, J. F., and Neve, R. L. (1988) *Nature 331*, 528−530.
14. Van Nostrand, W. E., Wagner, S. L., Suzuki, M., Choi, B. H., Farrow, J. S., Geddes, J. W., Cotman, C. W., and Cunningham, D. D. (1989) *Nature 341*, 546−549.
15. Van Nostrand, W. E., Wagner, S. L., Farrow, J. S., and Cunningham, D. D. (1990) *J. Biol. Chem. 265*, 9591−9594.
16. Schmaier, A. H., Dahl, L. D., Rozemuller, A. J. M., Roos, R. A. C., Wagner, S. L., Chung, R., and Van Nostrand, W. E. (1993) *J. Clin. Invest. 92*, 2540−2545.
17. Schmaier, A. H., Dahl, L. D., Hasan, A. A. K., Cines, D. B., and Van Nostrand, W. E. (1995) *Biochemistry 34*, 1171−1178.
18. Mahdi, F., Van Nostrand, W. E., and Schmaier, A. H. (1995) *J. Biol. Chem. 270*, 23468−23474.
19. Van Nostrand, W. E., Schmaier, A. H., Farrow, J. S., and Cunningham, D. D. (1990) *Science 248*, 745−748.
20. Bush, A. I., Martins, R. N., Rumble, B., Moir, R., Fuller, S., Milward, E., Currie, J., Ames, D., Weidemann, A., Fischer, P., Multhaup, G., Beyreuther, K., and Masters, C. L. (1990) *J. Biol. Chem. 265*, 15977−15983.
21. Van Nostrand, W. E., Schmaier, A. H., Farrow, J. S., Cines, D. B., and Cunningham, D. D. (1991) *Biochem. Biophys. Res. Commun. 175*, 15−21.
22. Van Nostrand, W. E., Schmaier, A. H., Farrow, J. S., and Cunningham, D. D. (1991*) Ann. N.Y. Acad. Sci. 640*, 140−144.
23. Maruyama, K., Ikeda, S., Ishihara, T., Allsop, D., and Yanagisawa, N. (1990) *Stroke 21*, 397−403.
24. Coria, F., Larrondo-Lillo, M., and Frangione, B. (1989) *J. Neuropathol. Exp. Neurol. 48*, 368−375.
25. Rozemuller, A. J. M., Roos, R. A. C., Bots, G. T. A. M., Kamphorst, W., Eikelenboom, P., and Van Nostrand, W. E. (1993) *Am. J. Pathol. 142*, 1449−1457.
26. Kawai, M., Kalaria, R. N., Cras, P., Siedlak, S. L., Velasco, M. E., Shelton, E. R., Chan, H. W., Greenberg, B. D., and Perry, G. (1993) *Brain Res. 623*, 142−146.
27. Kingston, I. B., Castro, M. J. M., and Anderson, S. A. (1995) *Nature Med. 1*, 138−142.
28. Van Nostrand, W. E., and Porter, M. (1999) *Biochemistry 38*, 11570−11576.
29. Burdick, D., Soreghan, B., Kwon, M., Kosmoski, J., Knauer, M., Henschen, A., Yates, J., Cotman, C., and Glabe, C. (1992) *J. Biol. Chem. 267*, 546−554.
30. Van Nostrand, W. E., Melchor, J., and Ruffini, L. (1997) *J. Neurochem. 69*, 216−223.
31. Wagner, S. L., Seigel, R. S., Vedvicke, T., Radschke, W. C., and Van Nostrand, W. E. (1992) *Biochem. Biophys. Res. Commun. 186*, 1138−1145.
32. Van Nostrand, W. E, Rozemuller, A. J. M., Chung, R., Cotman, C. W., and Saporito-Irwin, S. M. (1994) *Amyloid 1*, 1−7.
33. Bradford, M. M. (1976) *Anal. Biochem. 72*, 248−254.
34. Bieth, J. G. (1984) *Biochem. Med. 32*, 387−397.
35. Bush, A. I., Multhaup, G., Moir, R. D., Williamson, T. G., Small, D. H., Rumble, B., Pollwein, P., Beyreuther, K., and Masters, C. L. (1993) *J. Biol. Chem. 268*, 16109−16112.
36. Small, D. H., Nurcombe, V., Reed, G., Clarris, H., Moir, R., Beyreuther, K., and Masters, C. L. (1994) *J. Neurosci. 14*, 2117−2127.
37. Multhaup, G., Ruppert, T., Schlicksupp, A., Hesse, L., Bill, E., Pipkorn, R., Masters, C. L., and Beyreuther, K. (1998) *Biochemistry 37*, 7224−7230.
38. Cregg, J. M., Vedvick, T. S., and Raschke, W. C. (1993) *Bio/Technology 11*, 905−910.
39. Rossjohn, J., Cappai, R., Feil, S. C., Henry, A., McKinstry, W. J., Galatis, D., Hesse, L., Multhaup, G., Beyreuther, K., Masters, C. L., and Parker, M. W. (1999) *Nat. Struct. Biol. 6*, 327−331.
40. Van Nostrand, W. E. (1995) *Thromb. Res. 78*, 43−53.
41. Bornebroek, M., von dem Borne, P. A., Haan, J., Meijers, J. C. M., Van Nostrand, W. E., and Roos, R. A. C. (1998) *J. Neurol. 245*, 111−115.
42. Davis-Salinas, J., Saporito-Irwin, S. M., Cotman, C. W., and Van Nostrand, W. E. (1995) *J. Neurochem. 65*, 931−934.
43. Davis-Salinas, J., and Van Nostrand, W. E. (1995) *J. Biol. Chem. 270*, 20887−20890.
44. Davis, J., and Van Nostrand, W. E. (1996) *Proc. Natl. Acad. Sci. U.S.A. 93*, 2996−3000.
45. Davis, J., Cribbs, D. H., Cotman, C. W., and Van Nostrand, W. E. (1999) *Amyloid 6*, 157−164.
46. Mignatti, P., and Rifkin, D. B. (1993) *Physiol. Rev. 73*, 161−195.
47. Okumura, Y., Sato, H., Seiki, M., and Kido, H. (1997) *FEBS Lett. 402*, 181−184.
48. Mazzieri, R., Masiero, L., Zanetta, L., Monea, S., Onisto, M., Garbisa, S., and Mignatti, P. (1997) *EMBO J. 16*, 2319−2332.

BI0002840